ground water

Pure-Phase Transport and Dissolution of TCE in Sedimentary Rock Saprolite

by M. Lenczewski[1], L. McKay[2], A. Pitner[3], S. Driese[4], and V. Vulava[5]

Abstract

The objective of this study was to experimentally determine the influence of pore structure on the transport and dissolution of trichloroethylene (TCE) in clay-rich saprolite. In order to simulate a "spill," pure-phase TCE containing a water-insoluble fluorescent dye was injected into two heterogeneous 24-cm-diameter by 37-cm-long undisturbed columns of water-saturated saprolite. TCE entry occurred at capillary pressures of 2.7 and 4.0 kPa. Ten or 28 d after injection, the column was sliced horizontally into three sections and visually examined. The distribution of fluorescent dye indicated that pure-phase TCE migrated mainly through fractures in the shale saprolite and through fine root holes or other macropores in the limestone saprolite residuum. Analysis of saprolite subsamples indicated that TCE was present throughout much of the saprolite column but usually at concentrations less than the solubility of TCE. This spreading was caused by diffusion, which also contributed to the rapid dissolution of TCE in the fractures and macropores. Modeling was carried out using previously published dissolution and diffusion equations. The calculations confirm that rapid disappearance of immiscible TCE can occur in this type of material because of the small size of fracture or macropore openings and the high porosity of the fine-grained material. This study indicates that industrial solvents can readily enter fractures and macropores in otherwise very fine-grained subsoils and then rapidly dissolve and diffuse into the fine-pore structure, fromc which they may be very difficult to remove.

Introduction

Widespread industrial use of chlorinated solvents, such as trichloroethylene (TCE), has contributed significantly to ground water contamination problems in North America (National Research Council 1994; Pankow et al. 1996). These contaminants can enter the subsurface either as a solute or as a dense non–aqueous phase liquid (DNAPL), which may sink rapidly into the soil or rock and then slowly dissolve and spread through the ground water. Assessing the extent and fate of DNAPL contamination in materials containing fractures or macropores has proven to be particularly difficult. This is partly because migration of an immiscible DNAPL is strongly influenced by the characteristics of the fracture or macropore network, particularly the fracture aperture or the pore diameter, and their degree of interconnection (Kueper and McWhorter 1991). At the Oak Ridge Reservation (ORR) in East Tennessee, wastes containing dissolved or immiscible-phase DNAPLs were commonly buried in unlined trenches excavated into the clay-rich fractured saprolite. Saprolite is a fine-grained material consisting of thoroughly decomposed rock that retains some of its original structure and is widespread throughout the southeastern United States (Solomon et al. 1992; Driese et al. 2001). Relatively little is known about DNAPL behavior in this material. The experimental study described here focuses on entry of DNAPL into fractures or macropores

[1]Corresponding author: Department of Geology and Environmental Geosciences, Northern Illinois University, DeKalb, IL 60115; (815) 753-7937; fax (815) 753-1945; melissa@geol.niu.edu

[2]Department of Earth and Planetary Sciences, University of Tennessee, Knoxville, TN 37996; lmckay@utk.edu

[3]North Carolina Department of Environment and Natural Resources—Aquifer Protection, Section, Mooresville, NC 28115; andrew.pitner@ncmail.net

[4]Department of Geology, Baylor University, One Bear Place #97354 Waco, TX 76798; steven_driese@baylor.edu

[5]Department of Earth and Planetary Sciences, University of Tennessee, Knoxville, TN 37996; vulava@utk.edu

Received November 2004, accepted August 2005.

Copyright © 2005 The Author(s).
Journal compilation © 2006 National Ground Water Association.

doi: 10.1111/j.1745-6584.2005.00149.x

and its subsequent dissolution and diffusion into the fine-pore structure of the saprolite matrix.

To date, there have been very few experimental investigations of DNAPL behavior in clay-rich materials (examples include Hinsby et al. 1996; Cropper 1998; O'Hara et al. 2000; Lenczewski et al. 2004; Perfect et al. 2004), and many of these studies were carried out in glacial tills. The studies in till indicate that common DNAPLs, such as creosote and TCE, can readily penetrate many of the existing fractures under capillary pressures expected for even small spills (Hinsby et al. 1996; Jorgensen et al. 1998; O'Hara et al. 2000). These studies found that entry of DNAPL into fractures occurred at capillary pressures substantially lower than that predicted by the Corey (1986) equations, using "cubic law"–derived estimates of fracture aperture. This difference is at least partly because DNAPL entry pressure is controlled by the aperture of the largest fracture or macropore opening, while cubic law aperture values are calculated based on the bulk hydraulic conductivity and the fracture spacing, and hence are representative of the "average" aperture of all of the fractures (Snow 1969). In the only previous DNAPL experiment carried out in undisturbed saprolite, it was determined that entry of Fluorinert™ (solubility of 7 mg/L; relative density of 1.9) into fractures or macropores occurred at very low capillary pressures, ~10 cm of equivalent water head (Cropper 1998; Perfect et al. 2004). This confirmed that immiscible DNAPLs could penetrate the fractures or pores of some saprolite materials but did not address issues such as transport pathways, the influence of parent bedrock type, or the controls on dissolution of DNAPLs in saprolite.

Once a pure-phase DNAPL enters the water-saturated soil or rock it is subject to dissolution, which can proceed at widely variable rates. Parker et al. (1994, 1996) proposed that for soils or rocks with high matrix or primary porosity, dissolution of moderately soluble DNAPLs in fractures could occur relatively quickly (a few weeks to a few years) because of the large surface area to volume ratio of the DNAPL "body" and the strong concentration gradients between the pore water in the contaminated fractures and the pore water in the soil matrix. This rapid dissolution- and diffusion-controlled transfer of contaminant mass to the fine-grained matrix would make it impossible to remediate sites solely by pumping or otherwise removing the immiscible DNAPL. Removal of the dissolved contaminants would be very slow because they would have to diffuse back out of the matrix, greatly reducing the effectiveness of conventional pump-and-treat remediation systems and posing challenges for remediation strategies that attempt to deliver treatment to the matrix (McKay et al. 1993, 1997). The only experimental study to examine both immiscible DNAPL transport and subsequent dissolution in a fine-grained unlithified material was carried out by O'Hara et al. (2000). O'Hara injected TCE into a water-saturated column of fractured clay till from southern Ontario. Ten days after the injection of pure-phase TCE, the column was dismantled and the distribution of TCE was measured. The highest concentration of dissolved TCE was found only along portions of a few major fractures and in "haloes" of contamination several centimeters wide in the matrix adjacent to these fractures. These results were consistent with the DNAPL dissolution/matrix diffusion conceptual model posed by Parker et al. (1994, 1996) and indicate that for this geologic material, "spills" of pure-phase DNAPL should rapidly lead to spreading of dissolved contamination into the matrix.

The goal of this experiment was to determine if the conceptual model for free-phase DNAPL transport and dissolution in glacial tills (i.e., pure-phase transport in fractures and macropores, followed by rapid dissolution and diffusion into the fine-grained matrix) developed by Parker et al. (1994, 1996) and O'Hara et al. (2000) is also applicable to DNAPL spills in sedimentary rock saprolite. This study will experimentally determine whether (1) pure-phase TCE can penetrate fractures and/or macropores in saprolite under conditions typical of a small contaminant spill; (2) TCE transport and dissolution behavior differs according to the lithology of the parent bedrock of the saprolite (i.e., shale or limestone); and (3) dissolution and diffusion into the fine-grained matrix can play a significant role in redistribution of TCE contamination over the relatively short time spans (a few weeks) that might occur between the occurrence of a DNAPL spill and the implementation of an emergency DNAPL removal effort. The experimental results were then modeled to determine if the rapid disappearance was related to the pore structure. This research will aid in developing a better understanding of DNAPL transport and dissolution processes in saprolite, which is an important step needed for designing monitoring, containment, and remediation strategies.

Investigative Methods

Field Site

The column samples used in the experiment were collected at a depth of 1.5 to 1.9 m from sedimentary rock saprolite at Solid Waste Storage Area 7 (SWSA7) on the Department of Energy's ORR in eastern Tennessee. The column material is heterogeneous and consists of highly fractured and weathered saprolite derived from the Cambrian-age Dismal Gap Formation (Hatcher et al. 1992), typically with low organic matter ($f_{oc} = 0.001$ to 0.006; Jardine et al. 1989). The parent material is predominantly shale and limestone with smaller amounts of sandstone. Despite intense weathering, many of the characteristic structures, including bedding and two sets of cross-bedding fractures, are commonly preserved. Fracture spacing and aperture values are highly variable. Fracture spacing values in the upper 2 m of the saprolite range from 0.5 to 4.0 cm, and bulk hydraulic conductivity (K_{bulk}) values range from 4.5×10^{-9} to 2.7×10^{-4} m/s (Driese et al. 2001). Fracture aperture values calculated using the cubic law (Snow 1969) from the previously measured values of hydraulic conductivity and fracture spacing range from 19 to 110 μm (Driese et al. 2001).

Column Collection and Setup

Two columns were excavated and prepared following the methods of previous researchers (Jardine et al. 1988;

Harton 1996; Howard 1997; Cumbie and McKay 1999; Haun 1998) as modified by Cropper (1998) and Lenczewski et al. (2004) to make the casings and end caps solvent resistant. The columns were collected 1 m apart in the same pit at roughly the same depth (1.5 to 1.9 m). The samples were excavated in the shape of a cylinder with hand tools to keep disturbance to a minimum. Polyvinyl chloride pipe (25 cm diameter) was fitted over each saprolite column, and the annulus was filled with solvent-resistant epoxy (Ciba RP6401 Resin and Hardener and Ciba UREOL 5075 Resin and 6414 Hardener, for columns 1 and 2, respectively). After collection, the columns were trimmed in preparation for fitting with solvent-resistant end caps, resulting in column lengths of 37 cm and diameters of ~23 to 25 cm (Figure 1). The columns were placed in a 12°C chamber to simulate in situ conditions. A high–hydraulic conductivity sand layer was placed at the influent and effluent ends to allow for even spreading across the whole area of the column. The total volume in the tubing and end caps was ~40 mL. Each sample was then saturated with simulated Oak Ridge ground water (0.05 M $CaCl_2$) from the bottom inlet port to allow for any entrapped air to be removed prior to TCE injection. A constant-rate saturated flow test with measurements of head loss by pressure transducers was carried out to measure hydraulic conductivity prior to the TCE experiments. Samples of undisturbed peds of saprolite were collected from the excavation at the same depth as the columns for measurement of bulk density and total porosity using the wax clod method (Blake and Hartge 1986).

Injection of TCE

After the columns and tubing were completely saturated with artificial ground water and the hydraulic conductivity measurements were completed, the injection of pure-phase TCE began. Prior to injection, the pure-phase TCE was dyed (1 g per 100 mL of TCE) with Nile red (Sigma, St. Louis, Missouri), a fluorescent dye that is soluble in TCE but insoluble in water. The dyed TCE was then slowly pumped into each water-saturated column from the top using a high-precision digital screw pump (GDS Instruments Ltd., England) attached to a computer controller and data logger. Pressure transducers in the pump and at both the top and bottom of the column were used to monitor pressure during the injection. Pressure was stepped up by increments of 100 to 200 Pa. Volume of TCE injected was monitored at the pump (Figure 1). A clear glass sump was installed in the effluent line, just below the column, so that the time of first arrival of the red-dyed TCE could be observed. This occurred at day 26 for column 1 and day 4 for column 2. At this point, the TCE injection in each column was stopped and the columns were "shut in" (allowed to sit) for 28 d for the first column and 10 d for the second column to allow for dissolution and diffusion to occur before the columns were dismantled and sampled.

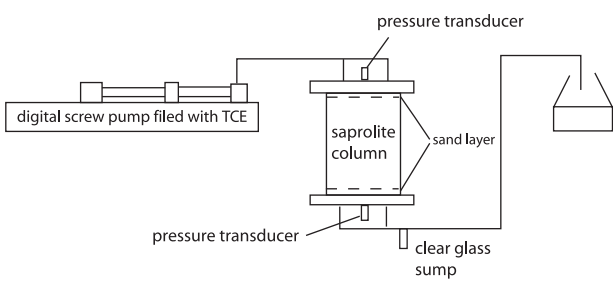

Figure 1. Schematic of the laboratory setup for the column experiments. The two saprolite columns collected allowed for different diffusion times (10 vs. 28 d) and the opportunity to examine the effects of heterogeneities in the saprolite.

Mapping of Contaminant Distribution and Lithologic Features

After the shut-in period of 28 d for the first column and 10 d for the second, each column was dismantled by cutting it into three disks, each 9 cm high. After carefully cleaning away any smeared material, the end of each slice of the saprolite column was photographed under both fluorescent lights and short-wave ultraviolet (UV) light. In addition to the photographs, observations about saprolite lithology, fracture and macropore distribution, and the distribution of the dye were noted. Saprolite lithology and fracture distribution were described following the methods used by Driese et al. (2001).

Shortly after the photographs were taken, the face of each slice was sampled using a microcoring technique developed by O'Hara et al. (2000), as shown in Figure 2. On average, 268 samples were taken on a grid system for each slice. Each cylindrical sample was 0.6 cm in diameter and ~1.25 to 2 cm long. Each microcore sample was weighed to determine the exact mass. Each sample was immediately extruded into a 15-mL centrifuge vial containing 5 mL of methanol. The capped vials were sealed to minimize volatilization, shaken, and placed in a 5°C refrigerator. Samples were processed to determine TCE content within 4 to 21 d of sampling by dilution with pentane and analysis on a Shimadzu GC-14A gas chromatograph equipped with an electron capture detector. The inlet temperature in the gas chromatograph was 180°C, and in the detector it was 300°C. The column temperature was held initially at 35°C for 5 min and then increased at a rate of 5°C/min to a final temperature of 90°C, which was maintained for 2 min.

After microcoring, the saprolite from column 2, slice 2 was allowed to completely air dry in a fume hood for preparation of thin sections as described in Mora et al. (1993). Thin sections were prepared for samples of both the limestone saprolite and the siltstone/shale saprolite, which were present in both of the columns. Microscopic analysis was conducted using standard soil petrographic techniques (FitzPatrick 1993). Apparent pore diameters were measured from the thin sections using a micrometer eyepiece attached to a standard petrographic microscope.

Results

Hydraulic Conductivity and Porosity

Bulk hydraulic conductivity (K_{bulk}) values of 2.11×10^{-7} and 5.56×10^{-6} m/s for columns 1 and 2, respectively, were determined from flow tests carried out prior

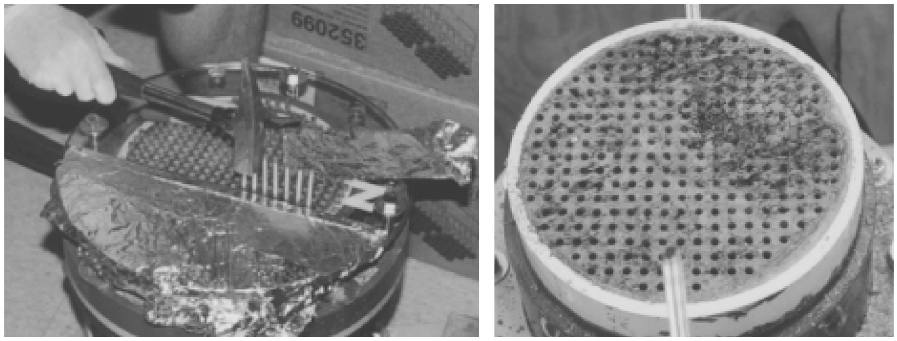

Figure 2. Collection of microcore samples and an example of grid pattern sampling on the face of a horizontal slice of a column. Each sampling point was 1.25 cm apart, and each sample was ~0.6 cm in diameter and 1.25 to 2 cm deep.

to TCE injection. These values are near the low end of the range of hydraulic conductivities obtained in other column experiments in the upper 2 m of saprolite at the SWSA7 site (Driese et al. 2001). Porosity values ranged from 33% to 62% with an average porosity of 50%, as determined from tests on 16 peds collected from the same depth in the pit as the columns. The peds used for porosity measurements typically did not contain major fractures or root holes; hence, the values represent the porosity of the fine-grained matrix.

TCE Capillary Pressure–Volume Measurements

To obtain capillary pressures, the dyed TCE was injected into the saprolite by gradually stepping up the pressure and measuring the volume of TCE introduced and the volume of water displaced from the column. A detailed discussion of the challenges of measuring capillary pressures in tall soil columns is presented in Perfect et al. (2004).

For column 1, the injection lasted just under 28 d before dyed immiscible TCE was detected in the sump of the effluent line (Figure 3A). During the first 8 d, the pressure was increased 100 Pa approximately every 8 h. During this time, 15 mL of TCE was injected. From 8 to 13 d the pressure was held constant at 3000 Pa, with only a few milliliters of additional TCE injected. On day 13, the pressure was increased to 3500 Pa, which was maintained until day 19. At this point, a total of <40 mL of TCE had been injected. This volume of TCE was accommodated mainly within the piping between the pump, the column, and the top end cap of the column without actual entry into the saprolite. At the beginning of day 20, the injection pressure was increased to 4000 Pa and after ~24 h there was a sharp rise in volume of TCE injected. The volume of TCE injected continued to increase for the next 8 d, indicating that the capillary pressure exceeded the entry pressure of many of the fractures or macropores. A final increase to 4500 Pa occurred on day 27, and dyed TCE was found in the sump in the effluent line the next day. For column 1, a total of 368 mL of dyed TCE was injected.

In contrast to column 1, the injection in column 2 was carried out much faster, lasting just under 4 d (Figure 3B). The injection was initiated with pressure increases of 250 Pa occurring approximately every 6 h. Entry of TCE into the saprolite column occurred at 2500 Pa, at the beginning of day 2, when there was a large increase in volume injected of ~110 mL. This was a volume greater than the volume expected to fill the piping and top end cap. This pressure was maintained for a day with no significant additional volume injected after the initial increase. Pressure increases to 2750 Pa and then to 3000 Pa resulted in continuous flow into the column until the dyed TCE was found in the effluent line at the end of day 3. This stepwise sequence of TCE injection suggests that the immiscible TCE initially entered some of the fractures or macropores at a pressure of 2500 Pa but then encountered a significantly smaller aperture fracture/macropore at an unknown depth (and therefore unknown

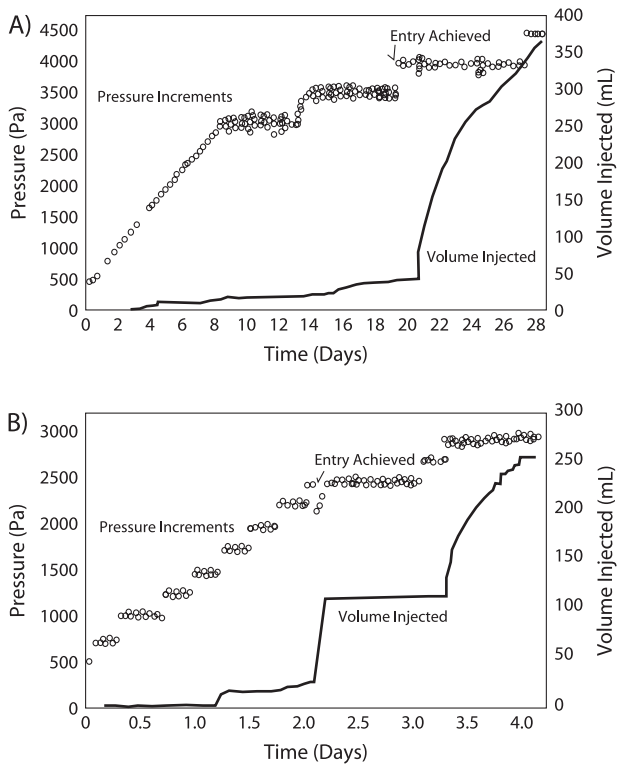

Figure 3. Injection pressure measured in the TCE at the top of the columns and dyed TCE volume injected for column 1 (A) and column 2 (B). Columns were saturated with water prior to injection of TCE.

aperture) within the column, which stopped the flow. Then, as capillary pressure was increased, the entry pressure for this constriction was exceeded and flow continued. For column 2, a total of 278 mL of dyed TCE was injected from the pump.

Lithology Determination

The lithologic characteristics and pore structure of the materials in each column were examined in detail to determine whether there were potential large aperture/opening pathways for immiscible TCE migration and to assess the possible origin of these pathways. Both columns were dominated by the clay-rich limestone residuum (31% to 50%) and the siltstone/shale saprolite (44% to 64%) with relatively little sandstone saprolite (5% to 6%). The micromorphology of the three principal saprolite lithologies was determined by thin section microscopy. The first is fragmental siltstone/shale saprolite comprising equal proportions of 0.5- to 5-cm diameter, angular to subangular, weathered saprolite fragments and a finer "matrix" within which the saprolite fragments are embedded. Macropores occur as irregular "shelters" formed by connections between saprolite fragments, which range from 50 to 500 μm in diameter.

The second type is limestone-derived saprolite residuum, which generally does not retain bedding structure from the parent bedrock. This has very high clay content and abundant root macropores that are primarily in the 50- to 500-μm size range, although many are partly infilled with fine-grained material. The abundance of plant roots in this type of material is probably related to a higher clay content and greater ease of root penetration. Several of the largest root pores were coated and/or plugged with the solvent-resistant resin used in preparing the columns for the TCE migration experiments; this resin was colored red in the thin sections by the dye that was used to help trace the flow paths of the pure-phase TCE. These largest root pores apparently extended from the annulus of the column (the source of the solvent-resistant resin) to at least 10 to 15 cm into the center of the column where the thin sections were prepared. The third saprolite type consists of interbedded sandstone, siltstone, and shale in which all of the primary rock layering is preserved but the rock is thoroughly decalcified. Sandstone-siltstone-shale saprolite lithologies are characterized by numerous macropores primarily in the 10- to 1000-μm size range, which originated through the dissolution of calcite spar cement-filled tectonic fractures. The fractures are spaced from 1 to 1.5 cm and are oriented both parallel and perpendicular to bedding. Fractures are coated with pedogenic clay and Fe/Mn oxides, which reduces the size of the pores and occludes some pores completely (Driese et al. 2001). Haloes of Fe reduction and Fe oxidation surround some fracture pores and indicate changing redox conditions during fluid flow through pores. Root pores are nearly absent in these lithologies and only occur rarely within clay-filled fractures. Based on these observations, it is clear that all three lithologies contain numerous fractures and/or root pores or dissolution pores that could act as pathways for TCE migration.

Distribution of TCE

As the immiscible-phase TCE dissolved and diffused into the matrix, the water-insoluble fluorescent dye was left as a residue on the surfaces of the fractures and macropores (Figure 4B). This provides direct evidence that the fractures and macropores served as preferential flow paths for immiscible TCE, although it provides no indication of the volume of TCE that flowed through these regions. Dye was found in both the blocky siltstone/shale saprolite and the limestone residuum typically along features that also had redox staining (Figure 4B), with the greatest intensity often occurring near the shale/limestone contacts. In the sandstone saprolite, dye was not observed. The dye in the siltstone/shale saprolite stained only the surface of fractures with a thin coating that could be scraped off. This indicates that immiscible TCE entered the fractures that separated blocks of matrix material, without penetration of the matrix. Based on the distribution of the dye, it is estimated that <20% of the fractures in the siltstone/shale saprolite were conducive to flow of TCE. The fluorescence in the clay-rich limestone saprolite was characterized by numerous scattered small points of dye, some occurring in clusters and others as isolated "hot" points. These features suggest that pure-phase TCE flow in the clay-rich limestone saprolite was primarily through macropores (probably fine root holes) and not through the fractures. When the columns were dismantled, the only locations where droplets of dyed pure-phase TCE were visible were at the ends. There was no evidence of artificial fracturing caused by the injection, or bypass flow between the soil column and the epoxy liner.

Concentrations of TCE in the microcore samples from column 2 are shown as contour plots on Figure 4C. The values are expressed relative to the solubility of TCE in water ($C_0 = 1100$ mg/L), assuming that all of the TCE was present in the water phase, even though individual samples may contain dissolved, sorbed and pure-phase TCE. Sorption parameters were not measured for this material, but a retardation factor (R) of 1.3 to 2.9 was estimated based on prior measurements of organic carbon content in the B horizon of similar soils at a nearby site ($f_{oc} = 0.001$ to 0.006; Jardine et al. 1989) and a typical distribution coefficient for TCE in organic matter of 117 L/kg (Fetter 1999). We have assumed that relative concentrations >1 indicate the likelihood of the presence of pure-phase TCE in a sample. If sorption is also considered, the area of each column slice expected to contain pure-phase TCE decreases slightly. As shown in Figure 4C, measurable amounts of TCE were found throughout all of column 2 (aged 10 d), with ~8% to 30% of the area of the slices having concentrations indicative of the presence of pure-phase TCE. The TCE concentrations decreased substantially with depth, which was consistent with the visual observations of the distribution of Nile red dye. The distribution of TCE concentrations in column 1 (aged 28 d; Pitner 2000) showed similar trends with depth, although the areas with relative concentrations >1 were smaller, ranging from 2% to 26% of each slice.

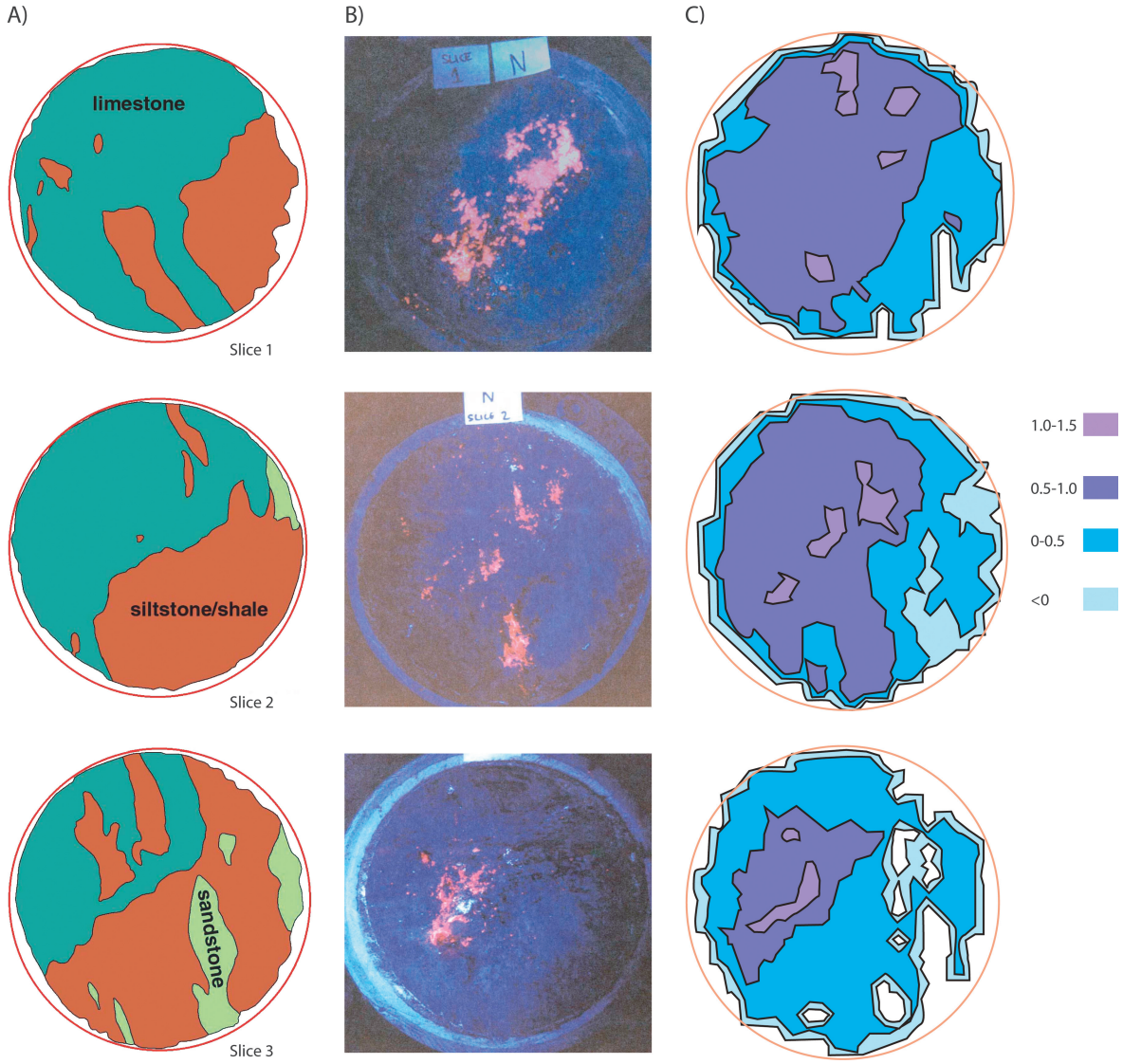

Figure 4. Column 2 (A) saprolite lithologic map, (B) short-wave UV light, and (C) relative concentration of TCE in the water phase (C/C_0 where $C_0 = 1100$ mg/L).

Discussion

Transport of Immiscible TCE

After a spill of pure-phase DNAPL in a fractured saprolite, transport occurs first through the largest-diameter macropores or largest-aperture fractures. In the field, it is hard to distinguish these large open macropores/fractures from similar features that have been infilled with pedogenic clays or are closed because of in situ stress conditions. However, in this study, open macropores/fractures were easily determined visually based on the residue of a fluorescent dye (Nile red) that was mixed with the pure-phase TCE. Examination of the saprolite after the dyed TCE spill indicated that conductive fractures/macropores were far more common than originally expected (Figure 4B). This is particularly true in the limestone saprolite residuum, which in the field or in hand specimen appears to be relatively homogeneous, with very few root holes or other macropores. In fact, the limestone residuum was just as conductive of immiscible TCE as the shale saprolite. The absence of dye in the sandstone saprolite was surprising because some fractures were observed in thin sections from this lithology. However, these fractures may have been much smaller in the column but opened during drying and preparation of the thin sections.

The size of the first fractures or macropores invaded by TCE in each column was calculated based on the measured entry pressures at the top of the column and the interfacial tension between TCE and water, σ, using the following equations from Corey (1986):

$$2b = \frac{2\sigma\cos\theta}{P_e} \text{ for fractures} \quad (1)$$

$$d = \frac{4\sigma\cos\theta}{P_e} \text{ for circular pores} \quad (2)$$

where $2b$ is the fracture aperture and d is the diameter of a circular pore, P_e is entry pressure into fracture or macropore, and θ is the contact angle between TCE and the mineral surfaces. Interfacial tension (σ) values for TCE,

ranging from 3×10^{-2} to 4×10^{-2} N/m, are reported in various sources (e.g., Demond and Lindner 1993; Harrold et al. 2003; Seo and McCray 2002). A σ value of 3.5×10^{-2} N/m was used for these calculations. In geologic materials containing low amounts of organic material, such as saprolite, water is typically assumed to be perfectly wetting (i.e., $\theta = 0$) relative to TCE and other similar nonpolar or weakly polar organic solvents (McWhorter and Kueper 1996; O'Hara et al. 2000; Perfect et al. 2004). Recently, Harrold et al. (2001) reported contact angles in the range of 20° to 45° for lab grade TCE on sandstone. To account for this uncertainty, we used θ values of 0° and 45° in the following calculations. Based on the measured entry pressures, the potential size of the largest fracture or root hole at the top of column 1 ranges between 12- and 18-μm aperture or 25- to 35-μm diameter, respectively. For column 2, the largest fracture or root hole sizes range between 20 and 28 μm or 40 and 56 μm, respectively. This calculation is only valid at the top of the column, where the capillary pressure was measured. As the TCE migrated deeper into the column, capillary pressures would increase, allowing entry into smaller fractures and macropores. The previous calculations are only valid for pure TCE. Uncertainty is expected to be much greater for DNAPL mixtures that occur in the field because of the large range in interfacial tension values and contact angles typically observed in these DNAPL mixtures (e.g., Harrold et al. 2001, 2003; Seo and McCray 2002).

A second estimate of fracture apertures ($2b$) was made using the cubic law (Snow 1969; as modified by McKay et al. 1993):

$$2b = \left[\frac{(K_{\text{bulk}} - K_{\text{matrix}}) \cdot 2B \cdot 12\mu}{\rho \cdot \text{g}}\right]^{1/3} \tag{3}$$

where K_{bulk} is the measured bulk hydraulic conductivity, $2B$ is the average fracture spacing (~1 cm), μ is the dynamic viscosity of water (1.2363 g/m s), K_{matrix} is 6.5×10^{-9} m/s (based on Wilson et al. 1992, for the same site), ρ is density of water at 12°C, and g is acceleration due to gravity. This equation assumes flow through the fractures is analogous to laminar flow between an orthogonal network of equal-aperture, continuous vertical fractures.

Based on this equation, calculated fracture aperture ($2b$) values for columns 1 and 2 were 15 and 44 μm, respectively, which are similar to the values obtained from TCE entry (12 to 28 μm). This suggests that cubic law aperture values, which are calculated based on parameters (bulk hydraulic conductivity and fracture spacing) that are relatively easy to measure could potentially be used to provide a preliminary assessment of whether a DNAPL will enter a fractured material for a given capillary pressure or depth of DNAPL spill. However, this assessment should be used cautiously because the cubic law assumes that all fractures in the sample have the same constant aperture, and hence the equation provides an estimate of the "typical" fracture aperture, whereas DNAPL entry is controlled by the largest fractures.

Uncertainty in bulk hydraulic conductivity (K_{bulk}) is also important because it can vary over 3 to 4 orders of magnitude in clay-rich saprolite (Driese et al. 2001). Uncertainty in the value of matrix hydraulic conductivity (K_{matrix}) is much less important, provided that it is substantially lower than K_{bulk}. For example, in this study, reducing the value of K_{matrix} from 6.5×10^{-9} to zero causes the calculated hydraulic aperture values ($2b$) for columns 1 and 2 to increase by only 1% and 0.02%, respectively. The value of fracture spacing ($2B$) can also influence hydraulic aperture values, but it is usually possible to directly measure this parameter. Even if there is uncertainty in the fracture spacing measurement, it usually does not have a large influence on the calculation because the hydraulic aperture varies according to the cube root of $2B$. In this study, varying $2B$ by a factor of 2 only changes the calculated fracture aperture values by 20% to 27% for the two columns.

Dissolution and Diffusion of TCE

Once the TCE entered the fractures, the processes of dissolution and diffusion were most likely responsible for the spreading of contamination away from the discrete flow paths identified by the dye. This process occurred over a relatively short period of time (10 or 28 d). The theoretical disappearance time, t_{D}, needed for complete dissolution and diffusion of immiscible-phase TCE from fractures was calculated for this experiment by using an equation and values presented by Parker et al. (1996, 1997) for a single parallel plate fracture:

$$t_{\text{D}} = \frac{\pi\rho^2}{16 S_{\text{w}}^2 \phi_{\text{m}}^2 D_{\text{e}} R}(2b)^2 \tag{4}$$

In this equation, ρ is the density of the DNAPL (TCE has density of 1.46 g/cm^3), S_{w} refers to the solubility of the DNAPL in water (1100 mg/L), ϕ_m refers to the matrix porosity (35%), D_{e} refers to the effective diffusion coefficient (estimated as 3.3×10^{-6} cm^2/s in Parker et al. 1996), R is the retardation factor (estimated values range from 1.3 to 2.9), and $2b$ is the fracture aperture. Fracture aperture values were determined from the entry pressure calculations (Equation 1), which were 12 to 18 μm for column 1 and 20 to 28 μm for column 2. Calculations using the previous parameters indicate that immiscible TCE would completely disappear in 5 to 21 d from column 1 and in 12 to 55 d from column 2. These calculations are consistent with the observed concentration distributions in columns 1 and 2, which showed that much, but not all, of the pure-phase TCE had dissolved within 10 to 28 d.

The distance or the width of the diffusion halo can be calculated using Devlin's (1994) adaptation of Crank's (1956) one-dimensional analytic solution to Fick's second law for a reactive solute:

$$\frac{C}{C_0} = \text{erfc}\left[\frac{x}{2\left(\frac{D_e t}{R}\right)^{0.5}}\right] \tag{5}$$

where C/C_0 is a ratio of the original concentration at distance x from the source at a time t, erfc is the

complementary error function, R is the retardation factor, and D_e is the effective diffusion coefficient. Using a TCE concentration of 11 mg/L, which is 1% of the aqueous solubility, and a 10-d isolation period, diffusion should carry this level of contamination 3.6 to 5.4 cm from a fracture, for retardation factors of 2.9 and 1.3, respectively. For a 28-d isolation period, the corresponding travel distances for the $C/C_0 = 1\%$ concentrations would be 6.0 to 9.0 cm. This simple calculation does not account for interference from TCE diffusing from nearby fractures, but it clearly demonstrates that diffusion at the scale of fracture spacing in the saprolite is a rapid process. The results are consistent with the observed concentration distributions that showed TCE had spread throughout the entire column, and the distribution was not just along prominent fractures or root holes.

Conclusions

The results of these experiments demonstrate that DNAPLs, such as TCE, can penetrate fractures and macropores in saprolite as a pure phase and then quickly dissolve and spread through the fine-pore structure by diffusion. The study suggests that even small DNAPL spills (a few centimeters of equivalent height of DNAPL pool) have the potential to penetrate fractures or root holes and contaminate large volumes of this material. The observed redistribution of TCE contamination over relatively short time spans (a few weeks) indicates that in the time between a typical DNAPL spill and the implementation of an emergency removal effort, much of the DNAPL will have already dissolved and entered the fine matrix pores. Although this may help to localize the contamination, it may also make it very difficult to remove using conventional remediation strategies, such as pump and treat, which tends to flush contaminants from the more highly conductive fractures or pores. Other remediation strategies, such as the introduction of bacteria or nutrients to aid in biodegradation of contaminants may also be less effective, depending on whether they can be transported into the fine matrix, where much of the contaminant resides.

Acknowledgments

This research was funded by a major grant from the Department of Energy EMSP Program (Project Number 55083). The University of Tennessee Waste Management Research and Education Institute and the University of Tennessee Research Center of Excellence-Center for Environmental Biotechnology provided additional funding and material support. The authors thank Chris Knight and John Sanseverino for their assistance. The authors would also like to thank the reviewers, Alan Fryar and John McCray, for their insightful comments.

Editor's Note: The use of brand names in peer-reviewed papers is for identification purposes only and does not constitute endorsement by the authors, their employers, or the National Ground Water Association.

References

Blake, G.R., and K.H. Hartge. 1986. Bulk density. In *Methods of Soil Analysis, Part I—Physical and mineralogical methods*. Soil Science Society of America, Agronomy, Monologue 9 (2nd ed.), ed. A. Klute, 363–375. Madison, Wisconsin.

Corey, A.T. 1986. *Mechanics of Immiscible Fluids in Porous Media*. Littleton, Colorado: Water Resources Publications.

Crank, J. 1956. *The Mathematics of Diffusion*. New York: Oxford University Press.

Cropper, S.C. 1998. Experimental measurements of capillary pressure-saturation drainage of air and DNAPL in fractured shale saprolite. Masters thesis, Geological Sciences, University of Tennessee, Knoxville.

Cumbie, D.H., and L.D. McKay. 1999. Influence of diameter on particle transport in a fractured shale saprolite. *Journal of Contaminant Hydrology* 37, no. 1–2: 139–157.

Demond, A., and A. Lindner. 1993. Estimation of interfacial tension between organic liquids and water. *Environmental Science & Technology* 27, no. 12: 2318–2331.

Devlin, J.F. 1994. A simple and powerful method of parameter estimation using simplex optimization. *Ground Water* 32, no. 2: 323–327.

Driese, S., L.D. McKay, and C.P. Penfield. 2001. Lithologic and pedogenic influences on porosity distribution and ground water flow in fractured sedimentary sarpolite; a new application of environmental sedimentology. *Journal of Sedimentary Research* 71, no. 5: 843–857.

Fetter, C.W. 1999. *Contaminant Hydrogeology*, 2nd ed. Upper Saddle River, New Jersey: Prentice Hall.

FitzPatrick, E.A. 1993. Soil horizons. In *Selected Papers of the Meeting of Commission V of the ISSS*. Special issue, 20, 361–430. Giessen, Germany: Catena.

Harrold, G., D.C. Gooddy, D.N. Lerner, and S.A. Leharne. 2001. Wettability changes in trichloroethylene-contaminated sandstone. *Environmental Science & Technology* 35, no. 7: 1504–1510.

Harrold, G., D.C. Gooddy, S. Reid, D.N. Lerner, and S.A. Leharne. 2003. Changes in interfacial tension of chlorinated solvents following flow through U.K. soils and shallow aquifer material. *Environmental Science & Technology* 37, no. 9: 1919–1925.

Harton, A.D. 1996. Influence of flow rate on transport of bacteriophage in a column of highly weathered and fractured shale. Masters thesis, Geological Sciences, University of Tennessee, Knoxville.

Hatcher, R.D. Jr., P.J. Lemiszki, R.B. Dreier, R.H. Ketelle, R.R. Lee, D.A. Lietzke, W.M. McMaster, J.L. Foreman, and S.Y. Lee. 1992. Status report on the geology of the Oak Ridge Reservation. ORNL/TM-12074. Oak Ridge National Laboratory, Oak Ridge, Tennessee.

Haun, D.D.B. 1998. Influence of ionic strength and cation valence on transport of colloid-sized microspheres in fractured shale saprolite. Masters thesis, Geological Sciences, University of Tennessee, Knoxville.

Hinsby, K., L.D. McKay, P. Jorgensen, M. Lenczewski, and C.P. Gerba. 1996. Fracture aperture measurements and migration of solutes, viruses, and immiscible creosote in a column of clay-rich till. *Ground Water* 34, no. 6: 1065–1075.

Howard, K.M. 1997. Factors influencing transport behavior of polyfluorinated benzoic acids in a highly weathered shale saprolite. Masters thesis, Geological Sciences, University of Tennessee, Knoxville.

Jardine, P., N. Weber, and J. McCarthy. 1989. Mechanisms of dissolved organic carbon adsorption on soil. *Soil Science Society of America Journal* 53, no. 5: 1378–1385.

Jardine, P., G. Wilson, and R. Luxmoore. 1988. Modeling the transport of inorganic ions through undisturbed soil columns from two contrasting watersheds. *Soil Science Society of America Journal* 52, no. 5: 1252–1259.

Jorgensen, P.R., K. Broholm, T.O. Sonnenborg, and E. Arvin. 1998. DNAPL transport through macroporous, clayey till columns. *Ground Water* 36, no. 4: 651–660.

Kueper, B.H., and D.B. McWhorter. 1991. The behavior of dense, nonaqueous phase liquids in fractured clay and rock. *Ground Water* 29, no. 5: 716–728.

Lenczewski, M., L. McKay, and A. Layton. 2004. Biodegradation of TCE in fractured shale and saprolite. *Ground Water* 42, no. 4: 534–541.

McKay, L.D., J.A. Cherry, and R.W. Gillham. 1993. Field experiments in a fractured clay till: 1. Hydraulic conductivity and fracture aperture. *Water Resources Research* 29, no. 4: 1149–1162.

McKay, L.D., P.L. Stafford, and L.E. Toran. 1997. EPM modeling of a field-scale tritium tracer experiment in fractured, weathered shale. *Ground Water* 35, no. 6: 997–1007.

McWhorter, D., and B. Kueper. 1996. Mechanics and mathematics of the movement of dense non-aqueous phase liquids (DNAPL) in porous media [Chapter 3]. In *Dense Chlorinated Solvents and Other DNAPLs in Groundwater*, ed. J.F. Pankow and J.A. Cherry, 89–128. Portland, Oregon: Waterloo Press.

Mora, C.I., D.E. Fastovsky, and S.G. Driese. 1993. Geochemistry and Stable Isotopes of Paleosols: A short course manual for the Annual Meeting of the Geological Society of America Convention, Department of Geological Sciences, University of Tennessee, Studies in Geology No. 23. University of Tennessee, Knoxville, Tennessee.

National Research Council. 1994. *Alternatives for Ground Water Cleanup*. Washington, D.C.: National Academy Press.

O'Hara, S.K., B.L. Parker, P.R. Jorgensen, and J.A. Cherry. 2000. Trichloroethene DNAPL flow and mass distribution in naturally fractured clay: 1. Evidence of fracture variability. *Water Resources Research* 36, no. 1: 135–147.

Pankow, J.F., S. Feenstra, J.A. Cherry, and M.C. Ryan. 1996. Dense chlorinated solvents in groundwater: Background and history of the problem [Chapter 1]. In *Dense Chlorinated Solvents and Other DNAPLs in Groundwater*, ed. J.F. Pankow and J.A. Cherry. Portland, Oregon: Waterloo Press.

Parker, B.L., J.A. Cherry, and R.W. Gillham. 1996. The effects of molecular diffusion on DNAPL behavior in fractured porous media [Chapter 12]. In *Dense Chlorinated Solvents and Other DNAPLs in Groundwater*, ed. J.F. Pankow and J.A. Cherry. Portland, Oregon: Waterloo Press.

Parker, B.L., R.W. Gillham, and J.A. Cherry. 1994. Diffusive disappearance of immiscible-phase organic liquids in fractured geologic media. *Ground Water* 32, no. 5: 805–820.

Parker, B.L., D.B. McWhorter, and J.A. Cherry. 1997. Diffusive loss of non-aqueous phase organic solvents from idealized fracture networks in geologic media. *Ground Water* 35, no. 6: 1077–1088.

Perfect, E., L. McKay, S. Cropper, S. Driese, G. Kammerer, and J. Dane. 2004. Capillary pressure-saturation relations for saprolite: Scaling with and without correction for column height. *Vadose Zone Journal* 3, no. 2: 493–501.

Pitner, A. 2000. Experimental investigations of factors controlling the spread of DNAPL contamination in undisturbed columns of fractured saprolite. Masters thesis, Geological Sciences University of Tennessee, Knoxville.

Seo, H.S., and J.E. McCray. 2002. Interfacial tension of chlorinated aliphatic DNAPL mixtures as a function of organic phase composition. *Environmental Science & Technology* 36, no. 6: 1292–1298.

Snow, D.T. 1969. Anisotropic permeability of fractured media. *Water Resources Research* 5, no. 6: 1273–1289.

Solomon, D.K., G.K. Moore, L.E. Toran, R.B. Drier, and W.M. McMaster. 1992. Status report—A hydrologic framework for the Oak Ridge Reservation. Environmental Sciences Division Publication No. 3815. ORNL/TM-12026. Oak Ridge, Tennessee: Oak Ridge National Laboratory.

Wilson, G.V., P.M. Jardine, and J.P. Gwo. 1992. Modeling the hydraulic properties of a multiregion soil. *Soil Science Society of America Journal* 56, no. 6: 1731–1737.

Don't Let the Well Run Dry

You can make a difference in the life of others around the world in need of safe and plentiful supplies of ground water. Make your tax-deductible contribution today to the Developing World Fund of the National Ground Water Research and Educational Foundation.

Established in 1994, NGWREF is operated as a 501c(3) foundation by the National Ground Water Association and is focused on education, research, and other charitable activities related to a broader understanding of ground water.

national ground water
research and educational foundation

National Ground Water Research and Educational Foundation
601 Dempsey Road
Westerville, Ohio 43081
800 551.7379
800 898.7786 fax

www.ngwa.org/ngwef/ngwef.html